Stem Cell Research 17 (2016) 391–400

Contents lists available at ScienceDirect

Stem Cell Research

journal homepage: www.elsevier.com/locate/scr

# Notch hyper-activation drives trans-differentiation of hESC-derived endothelium

David Reichman [a], Limor Man [a], Laura Park [a], Raphael Lis [b], Jeannine Gerhardt [a], Zev Rosenwaks [a], Daylon James [a,b,*]

[a] Center for Reproductive Medicine and Infertility, Weill Cornell Medical College, New York, NY 10065, United States
[b] Tri-Institutional Stem Cell Derivation Laboratory, Weill Cornell Medical College, New York, NY 10065, United States

ARTICLE INFO

*Article history:*
Received 25 April 2016
Received in revised form 1 September 2016
Accepted 13 September 2016
Available online 13 September 2016

ABSTRACT

During development, endothelial cells (EC) display tissue-specific attributes that are unique to each vascular bed, as well as generic signaling mechanisms that are broadly applied to create a patent circulatory system. We have previously utilized human embryonic stem cells (hESC) to generate tissue-specific EC sub-types (Rafii et al., 2013) and identify pathways that govern growth and trans-differentiation potential of hESC-derived ECs (James et al., 2010). Here, we elucidate a novel Notch-dependent mechanism that induces endothelial to mesenchymal transition (EndMT) in confluent monolayer cultures of hESC-derived ECs. We demonstrate density-dependent induction of EndMT that can be rescued by the Notch signaling inhibitor DAPT and identify a positive feedback signaling mechanism in hESC-ECs whereby trans-activation of Notch by DLL4 ligand induces elevated expression and surface presentation of DLL4. Increased Notch activation in confluent hESC-EC monolayer cultures induces areas of EndMT containing transitional cells that are marked by increased Jagged1 expression and reduced Notch signal integration. Jagged1 loss of function in monolayer hESC-ECs induces accelerated feedback stimulation of Notch signaling, increased expression of cell-autonomous, cis-inhibitory DLL4, and EndMT. These data elucidate a novel interplay of Notch ligands in modulating pathway activation during both expansion and EndMT of hESC-derived ECs.



## 1. Introduction

The mammalian heart begins as a linear tube that is comprised to two cells types - myocardium, the muscle cells that drive mechanical function, and endocardium, the primary endothelial cell (EC) population (Harvey, 2002). In order to form a multi-chambered organ, the heart tube undergoes "looping" and endocardial cells undergo endothelial to mesenchymal transition (EndMT), migrate into the cardiac jelly and proliferate to form the cardiac valves and septum (von Gise and Pu, 2012). EndMT has long been thought to occur exclusively in the context of embryonic cardiogenesis, however, recent studies provide evidence for EndMT in adult tissues that is thought to contribute to the pathogenesis of many diseases, including pulmonary (Arciniegas et al., 2005), intestinal (Rieder et al., 2011), kidney (Zeisberg et al., 2008) and cardiac fibrosis (Zeisberg et al., 2007). As such, the molecular pathways that govern EndMT are not only relevant to basic studies of cardiogenesis, but also may enable targeted therapies that improve functional perfusion of diseased or injured tissues.

Multiple signaling pathways have been linked to EndMT, including transforming growth factor beta (TGFβ) (Gonzalez and Medici, 2014), nitric oxide (NO) (Chang et al., 2011), and fibroblast growth factor (FGF) (Chen et al., 2012), however, Notch signaling in known to play a central role in both the demarcation of boundaries within the embryonic vascular network (Benedito et al., 2009) as well as EndMT (Niessen and Karsan, 2008). The Notch family is comprised of four transmembrane receptors (Notch1–4) that are activated by membrane-anchored ligands Delta-like (DLL) 1, 3 and 4 and Jagged (JAG) 1 and 2. Notch ligand on one cell can trans-activate Notch receptor on neighboring cells, resulting in release of the Notch intracellular domain (NICD) via proteolytic processing and translocation to the nucleus to activate transcription of downstream targets such as HES and HEY (Guruharsha et al., 2012). Yet Notch ligands are also capable of inhibiting receptor activation in the cell they are presented on (cis-inhibition) (de Celis and Bray, 1997; Klein et al., 1997; Micchelli et al., 1997; Miller et al., 2009; Sprinzak et al., 2010). Differential activity between DLL and JAG ligands adds further nuance to Notch signaling; in cells expressing "fringe" genes (lunatic fringe, manic fringe or radical fringe), Notch receptors are modified such that DLL ligand strongly activates, but JAG ligand inhibits, signaling (Benedito et al., 2009). This many-tiered regulatory apparatus enables the formation of stark boundaries that are essential for

* Corresponding author at: Center for Reproductive Medicine and Infertility, Weill Cornell Medical College, New York, NY 10065, United States.
*E-mail address:* djj2001@med.cornell.edu (D. James).

http://dx.doi.org/10.1016/j.scr.2016.09.005

tissue morphogenesis. However, due to the complexity of Notch signal regulation, interpretation of phenotypes in transgenic mouse and in vitro gain/loss of function studies can be challenging.

Human embryonic stem cells (hESC) provide an accessible platform for modeling cardiovascular differentiation in vitro, thus permitting the interrogation of signaling pathways that are specifically active in embryonic endothelium. Moreover, hESC-derived ECs can recapitulate fundamental cellular events, like EndMT, that occur uniquely in developmental and/or pathological contexts. We have previously developed culture conditions that promote cardiovascular differentiation of hESCs and identified signaling pathways that affect trans-differentiation of hESC-derived ECs to mesenchymal fate (James et al., 2010). In this study, we generated hESC-derived ECs that exhibited multiple hallmarks of EndMT when sustained in monolayer culture. Phenotypic transition of hESC-ECs was Notch dependent, and mediated by a positive feedback circuit in which activation of Notch resulted in upregulation of DLL4 ligand and subsequent activation of Notch in neighboring cells. Upon reaching a critical threshold of Notch signal activation in high-density monolayer culture, EndMT was initiated in cells exhibiting increased surface expression of JAG1, which combined with elevated cis-expression of DLL4 to exert an inhibitory role on Notch activation. These findings expand upon the previously documented interplay

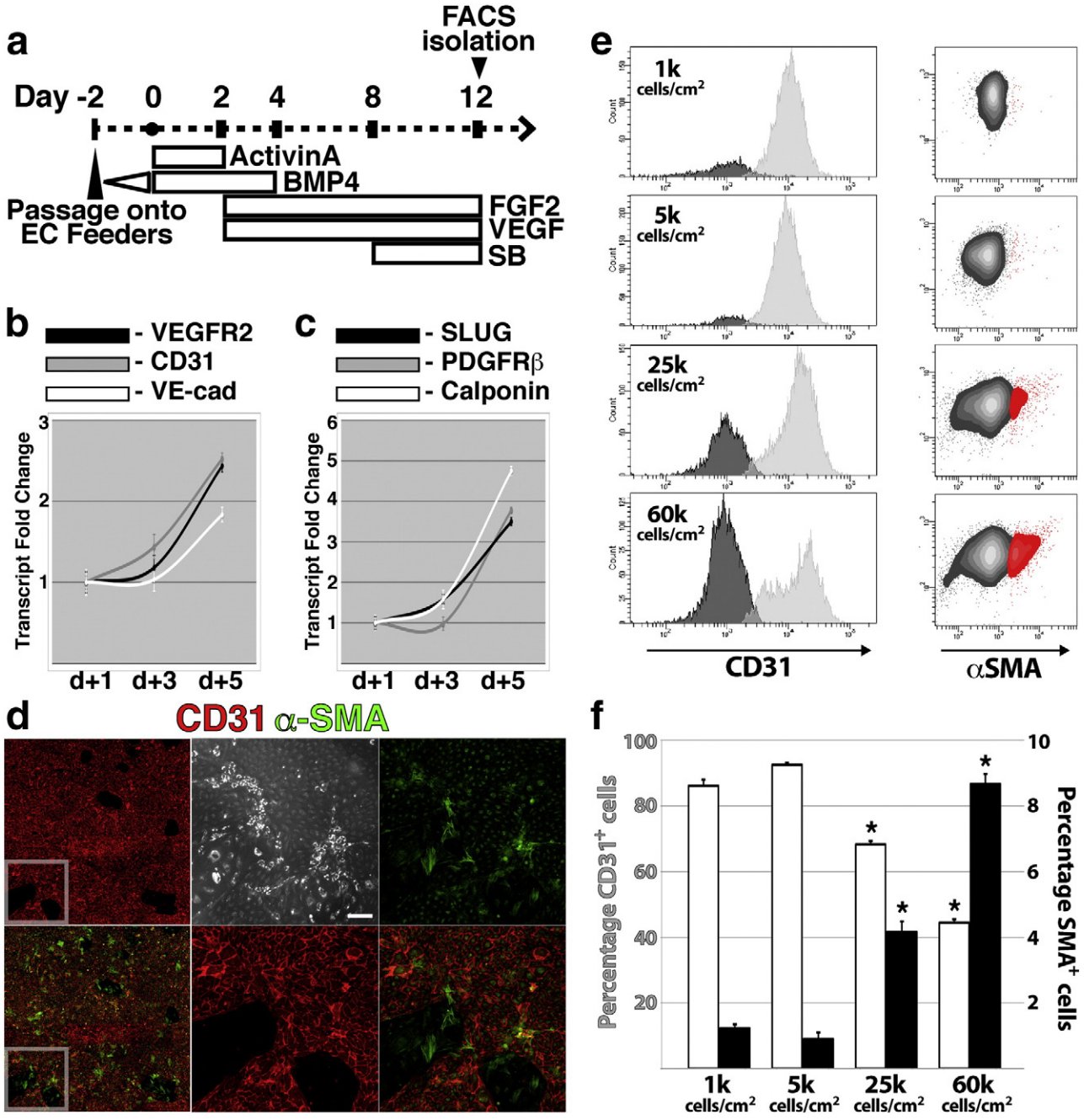


**Fig. 1.** hESC-derived ECs undergo EndMT in purified monolayer culture. (a) VPr-mOrange hESCs were subjected to a cardiovascular differentiation protocol on vascular feeders. (b and c) hESC-derived ECs were isolated by FACS following differentiation and cultured in monolayer; following 1, 3 and 5 days of culture, transcript levels were measured for genes related to EC identity (b) and EndMT (c). (d–f) hESC-ECs were isolated and plated at variable cell densities; EC cultures plated at high density were labeled with a fluorophore-conjugated antibody specific for α-SMA; (e and f) the percentage of α-SMA + cells was quantified in EC cultures plated at variable densities following 5 days of monolayer culture (e and f). Error bars in (b, c and f) represent standard deviation of experimental values performed in triplicate. Error bars in (b, c and f) represent standard deviation of experimental values performed in triplicate; * - $p < 0.01$ relative to 1 K and 5 K densities. The stroke box in (d) is shown at higher magnification at the right. Scale bar – 100 μm.

between Notch ligands in designating tip/stalk cell phenotype during vasculogenesis and integrate a novel signaling mechanism for EndMT in hESC-derived ECs.

## 2. Results

### 2.1. hESCs-derived ECs undergo EndMT in purified monolayer culture

We have previously developed tools for the robust differentiation and specific identification of ECs from hESCs (James et al., 2010; James et al., 2011). These studies revealed significant trans-differentiation potential of hESC-ECs, which was mitigated by inhibition of TGFβ signaling. To define the ontogeny of mesenchymal cells that emerge from hESC-ECs, we subjected hESCs to a cardiovascular differentiation protocol (Fig. 1a) and purified resultant ECs after 12 days for extended growth in monolayer culture. Transcriptional profiling of purified hESC-EC cultures at two day intervals beginning the day after initial plating revealed increased expression of EC-specific genes (Fig. 1b), as well as genes that have been linked to EndMT and pericytic identity (Fig. 1c). Staining for α-Smooth Muscle Actin (α-SMA) identified regions of EndMT that were evident as primary cultures reached confluence (Fig. 1d). Notably, increased initial plating density of hESC-ECs resulted in an elevated proportion of derivatives expressing α-SMA after 5 days (Fig. 1e and f). These data affirm the capacity for hESC-ECs to undergo EndMT and reveal initial plating density as a critical modulator of EC transdifferentiation.

### 2.2. Notch signal inhibition enhances yield and purity of hESC-derived ECs

Notch signaling, which is activated by membrane bound ligand/receptor interactions, is known to play a central role in EndMT during embryonic cardiogenesis, and was thus a likely mediator of EndMT in hESC-ECs. To assess the functional contribution of Notch signal activation to the EndMT of hESC-ECs, we differentiated hESCs in the presence of SB431542 and DAPT, small molecule inhibitors of TGFβ and Notch signaling, which are both known to play a role in EndMT. Inhibitors were added beginning at 8 days of differentiation and by day 14, addition of DAPT increased vascular density within organoid differentiation cultures (Fig. 2a). Flow cytometric analysis revealed that SB431542 increased the total number of hESC-derived cells, while DAPT increased the number and proportion of total ECs among hESC-derivatives (Fig. 2b). To determine when during differentiation Notch inhibition confers a benefit, we exposed cultures to DAPT during three discreet windows loosely correlating to mesoderm induction, vascular

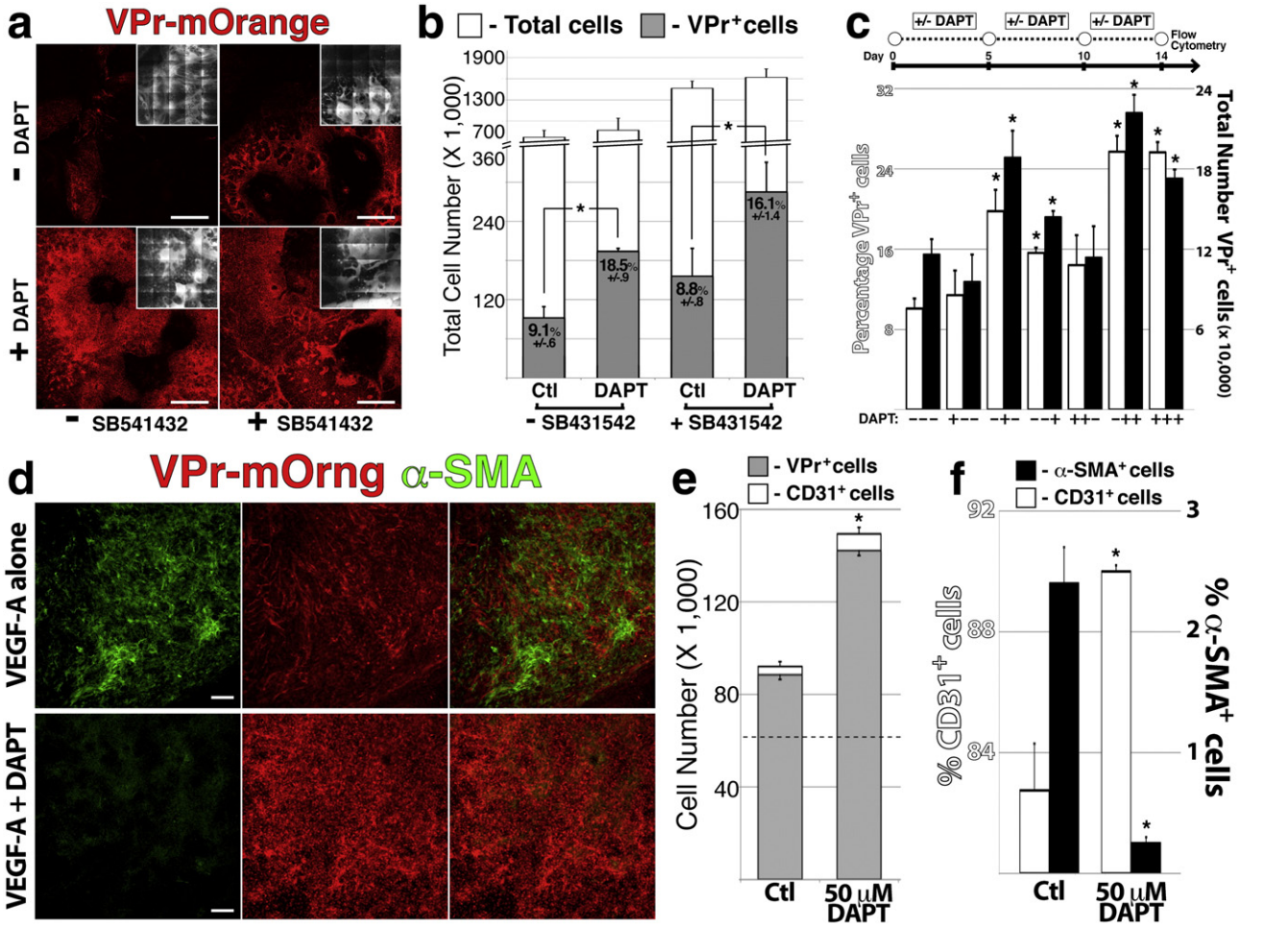


**Fig. 2.** Notch inhibition enhances yield and purity of hESC-derived ECs. (a and b) Beginning at 8 days of differentiation, VPr-mOrange hESCs were exposed to the Notch signal inhibitor DAPT and/or the ALK4/5/7 inhibitor SB431542; at day 14 representative confocal micrographs showed the extent of $VPr^+$ cells (a) and flow cytometry (b) quantified the relative distribution of ECs (black). (c) VPr-mOrange hESCs were differentiated with DAPT included in growth media within one or more temporal windows (days 0 to 5, days 5 to 10, or days 10 to 14); following 14 days the relative percentage (white) and number (black) of $VPr^+$ ECs in resultant cultures was measured by flow cytometry. (d) Day 14 cultures supplemented with VEGF-A alone, or VEGF-A and DAPT for days 5 to 14 were stained for α-SMA by immunofluorescence. (e and f) Following differentiation of VPr-mOrange hESCs in control conditions, the $VPr^+CD31^+$ EC population was purified by FACS and plated at an input of sixty thousand cells per well of a 6-well dish; following five days of growth in medium supplemented with VEGF-A alone or VEGF-A and DAPT, total EC number (e) and percentage of $CD31^+$ and $\alpha\text{-SMA}^+$ cells (f) was quantified by intracellular flow-cytometry. Error bars in (b, c, e and f) represent standard deviation of experimental values performed in triplicate; * - $p < 0.01$. The insets in (a) shows a brightfield view. Scale bar in (a) – 1 mm; scale bar in (d) – 100 μm.

specification and EC expansion/preservation (Fig. 2c). Both the percentage and number of VPr$^+$ ECs were enriched when DAPT was included during intermediate and late temporal windows. Under these growth conditions, immunofluorescence revealed few α-SMA$^+$ cells, while control cultures supplemented with VEGF-A alone exhibited widespread α-SMA$^+$ cells (Fig. 2d). Upon isolation and monolayer culture of VPr$^+$ ECs, supplementing growth medium with DAPT increased the overall number of ECs after 5 days (Fig. 2e), and increased the percentage of ECs in outgrowths at the expense of α-SMA$^+$ cells (Fig. 2f). Taken together, these data suggest that inhibition of Notch signaling increased the number and proportion of ECs in hESC differentiation cultures by promoting proliferation, and preserving vascular cell identity.

### 2.3. Transitional ECs exhibit increased JAG1 expression and reduced Notch activation

To define spatial distribution and expression levels of Notch ligands during EndMT, we used fluorophore-conjugated antibodies to localize DLL4 and JAG1 ligands in confluent monolayers of hESC-derived ECs (Fig. 3). Isolated α-SMA$^+$ derivatives of EndMT displayed elevated surface expression of JAG1 (Fig. 3a) and increased expression of PDGFRβ (Fig. 3b), with reduced nuclear localization of the Notch target HEY1 in JAG1$^{high}$ cells (Fig. 3c). To provide some indication of the level of Notch activation during EndMT, hESC-ECs were incubated for 30 min with fluorophore-conjugated antibodies against DLL4 and JAG1 in live cell cultures, then washed with PBS and returned to culture media. This enabled a crude measure of ligand internalization in signal-presenting cells and revealed that DLL4-mediated activation was reduced in transitional hESC-ECs, which displayed a VPr$^{low}$DLL4$^{neg}$JAG1$^{high}$ phenotype (Fig. 3d). Additionally, hESC-ECs surrounding zones of EndMT showed relatively reduced DLL4 internalization, suggesting that loss of DLL4 activity nucleated a wave of reduced Notch activation that radiated outward from transdifferentiating ECs. Immunocytochemistry revealed the cellular localization of Notch1 intracellular domain (Notch1 ICD), thus providing a surrogate measure of Notch pathway activation. Notch1 ICD was enriched in nuclei of subconfluent hESC-ECs (Fig. 3e), but was relatively reduced in nuclei of confluent or transitional hESC-ECs (Fig. 3f). To further assess the change in Notch signal activation upon transition to mesenchymal phenotype, the VPr$^+$CD31$^+$ and CD31$^{neg}$PDGFRβ$^+$ populations were FACS sorted from monolayer cultures following phenotypic transition and endothelial, mural and Notch-related transcripts were measured by qPCR (Fig. 3g). Relative to the CD31$^+$ fraction, PDGFRβ$^+$ cells showed markedly reduced (10–100 fold) levels of transcripts reflecting Notch activation (DLL4, NOTCH1, NOTCH4, HEY1) and EC identity (CD31, VEGFR2, CDH5), and increased levels of mural cell markers (CALPONIN, PDGFRβ) and SLUG, a key transcription factor governing EndMT.

### 2.4. Jagged1 knockdown induces accelerated Notch activation feedback and EndMT

The interplay of DLL4 and JAG1 in differential activation of Notch signaling has been previously noted (Benedito et al., 2009), with weak-acting JAG1 effectively inhibiting DLL4-mediated Notch activation in ECs expressing Fringe genes. To determine whether elevated surface expression of JAG1 in transitional ECs may reflect a competitive interplay between Notch ligands, we used multiple lentiviral shRNAs to target DLL4 and JAG1 gene products (Fig. 4 and Supplementary Fig. 1). Relative to control shRNA, DLL4 and JAG1 shRNAs reduced their targets at the transcript (Fig. 4a and Supplementary Fig. 1a) and protein (Fig. 4b–d) levels. Notably, while knockdown of DLL4 resulted in relatively less JAG1 transcript and protein, knockdown of JAG1 resulted in nearly two-fold increase in DLL4 transcript/protein. Knockdown of JAG1 also promoted increased NOTCH1 ICD nuclear enrichment, even in confluent hESC-EC cultures, and increased the frequency of CD31$^{neg}$ cells (Fig. 4e). Purified ECs treated with shRNAs (Fig. 4f and g) or DAPT (Fig. 4f) were analyzed by qPCR on successive days, revealing an accelerated elevation of DLL4, Notch1/4 and HEY1 transcripts in cells transduced with JAG1 shRNA (Fig. 4f). Notably, the transcript level of Jagged2 was elevated 3-fold in response to JAG1 shRNA, perhaps reflecting a compensatory function in these cells. Consistent with activation of Notch signaling being correlated with arterial identity, cells treated with DLL4 shRNA or DAPT showed reduced expression of the arterial surface marker EPHRINB2 while JAG1 shRNA induced a reduction in the venous transcription factor COUPTFII (Fig. 4g, left). Markers of mural cell identity (PDGFRβ, NOTCH3, CALPONIN) and EndMT (SLUG) were increased in response to JAG1 shRNA relative to controls (Fig. 4g, middle), and remained relatively low in DLL4 shRNA or DAPT-treated cells. Notably, effectors of TGFβ signaling were differentially regulated in response to JAG1 shRNA (Fig. 4g, right) – BMPER, which has been shown to antagonize BMP/GDF signaling (Moser et al., 2003), was minimally, though significantly increased, while endoglin, a co-receptor that enables activation of BMP/GDF signaling in response to TGFβ1 in ECs (Lebrin et al., 2004), was reduced. Finally, JAG1 shRNA induced elevated expression of GUCY1A3, GUCY1B3 and INHIBINA, which together with IGF2 enable nitric oxide signaling and EndMT in cardiac cushions downstream of Notch activation (Chang et al., 2011). Together, these data suggested a role for JAG1 in mitigating Notch signal activation in monolayer ECs, and demonstrated increased signaling feedback and EndMT following knockdown of JAG1.

### 2.5. Hyper-activation of Notch signaling promotes DLL4-mediated cis-inhibition and EndMT

Notch ligands are membrane bound, and ligand internalization by signal-presenting cells is an important factor in NICD internalization within the signal-receiving cell (Parks et al., 2000). Moreover, in signal-presenting cells ligands can inhibit, instead of activate, Notch receptors in a cell-autonomous fashion (cis-inhibition) (de Celis and Bray, 1997; Klein et al., 1997; Micchelli et al., 1997; Miller et al., 2009; Sprinzak et al., 2010). To define the relative contribution of cis- versus trans-presentation of Notch ligands to the phenotypes observed in our system, we specifically over-expressed DLL4 cDNA in a population of hESC-derived ECs and co-cultured these cells with an even input of cells that were clonally labeled with blue fluorescent protein (BFP, Fig. 5). Overexpression of DLL4 cDNA had a stark dose-dependent effect on the total cell number (Fig. 5a) and percent yield (Fig. 5b) of hESC-derived ECs, without an evident increase in apoptotic cells (data not shown). In combined monolayer cultures, the ratio of signal-receiving (SR, blue) to signal-presenting (SP, grey) was slightly skewed in favor of SR cells at all-time points, however, after 6 days, knockdown of JAG1 reduced cell number in SR cells, as well as in control SP cells

**Fig. 3.** Transitional ECs exhibit increased JAG1 expression and reduced Notch activation. (a and b) Following 5 (a) or 6 (d) days of growth in purified monolayer culture, hESC-ECs were labeled with fluorophore conjugated antibodies specific for CD31 (red), α-SMA (green), Jagged1 (blue) and PDGFRβ (grey). (c) Following 4 days hESC-ECs were labeled with fluorophore-conjugated antibodies specific for CD31 (red), Jagged1 (blue) and HEY1 (green). (d) Following 5 days of growth, fluorophore conjugated antibodies specific for DLL4 (green) and JAG1 (blue) were added directly to culture media at 37 °C; after 30 min, cells were washed three times with PBS, incubated with warm growth medium for 15 min at 37 °C and then imaged by confocal microscopy. (e and f) In sub-confluent (e) and confluent (f) cultures of hESC-ECs, cells were fixed and labeled with an antibody specific for the NOTCH1 intracellular domain and CD31; arrows in the inset indicate nuclei and asterisk in (f) shows CD31$^{neg}$ transitional cells. (g) Following 6 days, monolayers were dissociated and labeled with antibodies specific for CD31 and PDGFRβ; the CD31$^+$PDGFRβ$^{neg}$ and CD31$^{neg}$PDGFRβ$^+$ populations were sorted by FACS and qPCR analysis was performed for the genes shown. Error bars in (g) represent standard deviation of experimental values performed in triplicate; * - $p < 0.01$. Brightfield views are shown in (a and d). The stroke box in (c, e and f) is shown at higher magnification in the inset. Scale bars in (a–f) – 100 μm.

(Fig. 5c). Overexpression of DLL4 in SP cells induced a pronounced effect on DLL4 surface expression in SR cells, and knockdown of JAG1 magnified this effect (Fig. 5d). Quantification of $CD31^{+}$ and $CD31^{neg}$ cells in the SR population showed a decrease in total $CD31^{+}$ cells induced by overexpression of DLL4 in SP cells, and although high DLL4 in SP cells promoted a significant increase in $CD31^{neg}$ cells within the SR fraction,

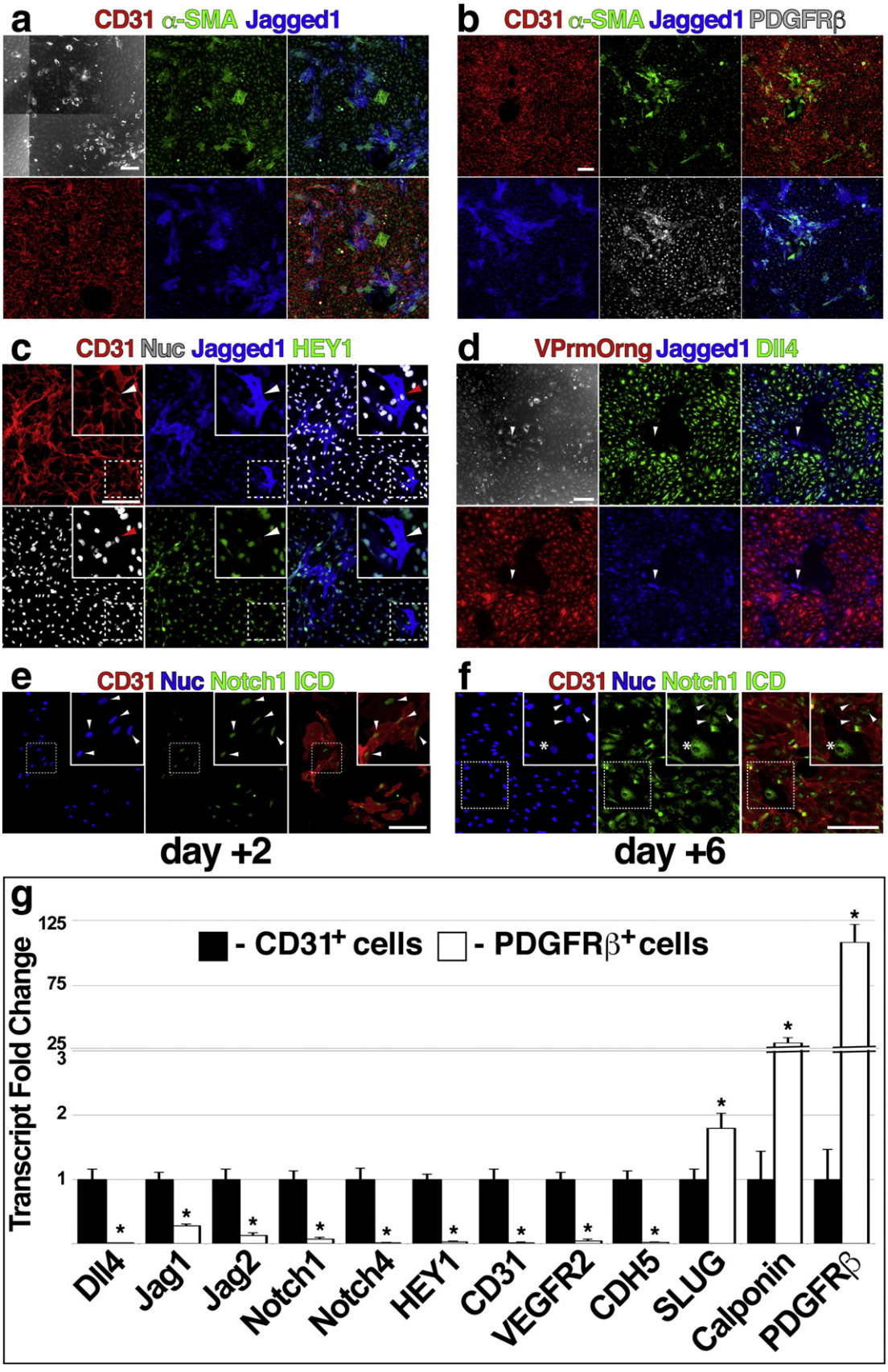

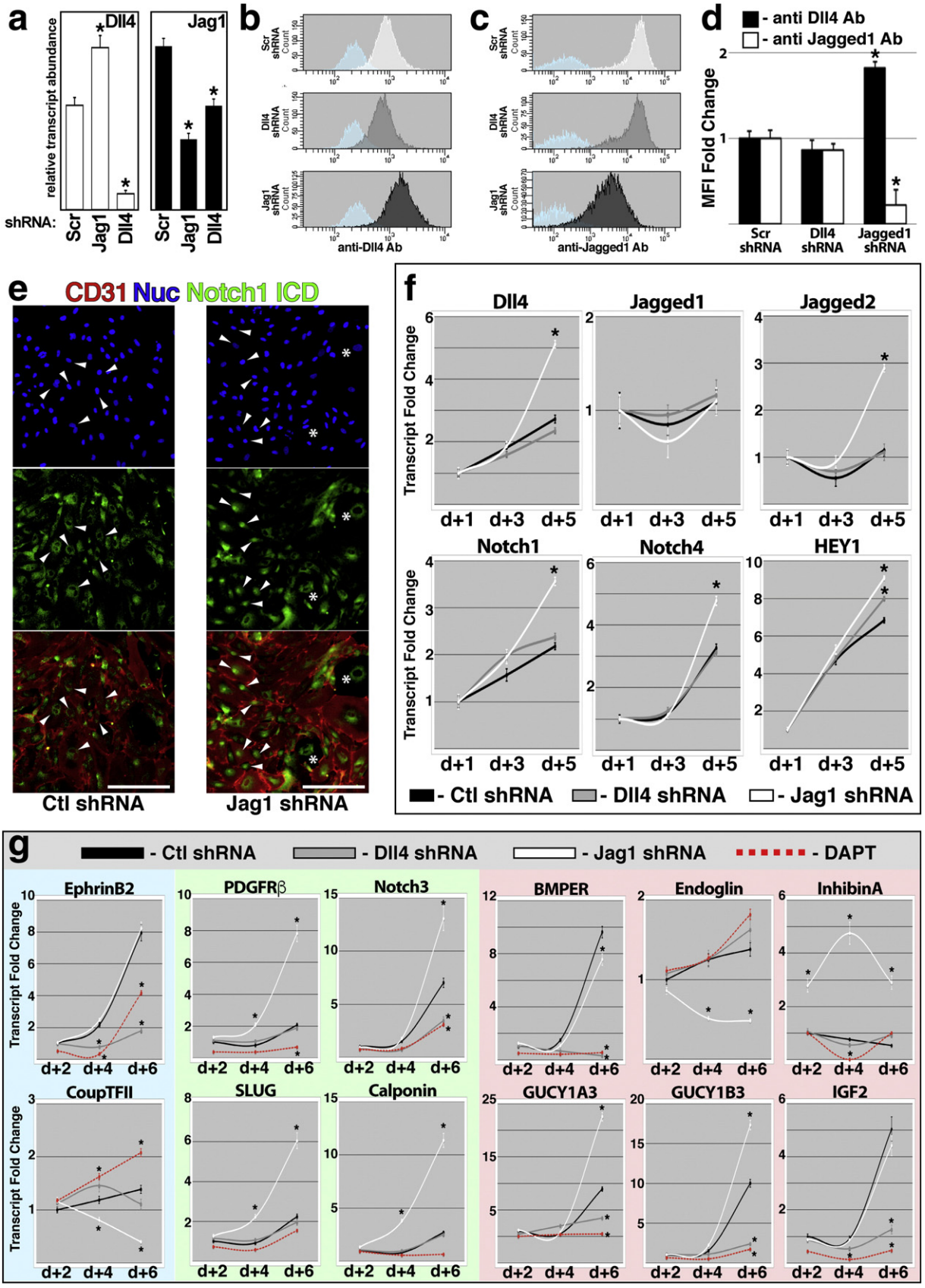


**Fig. 4.** Jagged1 knockdown induces accelerated Notch activation feedback and EndMT. (a–d) Control (Scrambled), JAG1 and DLL4 lentiviral shRNAs were added to hESC-ECs upon purification from day 14 differentiation cultures; following 5 days, qPCR (a) and flow cytometric analyses (b–d) of DLL4 (a, d and d) and JAG1 (a, c and d) were performed. (e) Confluent hESC-EC cultures that had been transduced with Control or JAG1 shRNA were labeled with antibodies specific for NOTCH1 intracellular domain and CD31; arrowheads indicate nuclei and asterisks show $CD31^{neg}$ transitional cells. (f) At 1, 3 and 5 days following addition of Control, DLL4 or JAG1 lentiviral shRNAs, transcriptional analysis of Notch related genes was performed by qPCR. (g) At 2, 4 and 6 days following addition of lentiviral shRNAs or DAPT, qPCR analysis was performed for the genes shown. Error bars in (a, d, f and g) represent standard deviation of experimental values performed in triplicate; * - $p < 0.01$. Scale bars in (e) – 100 μm.

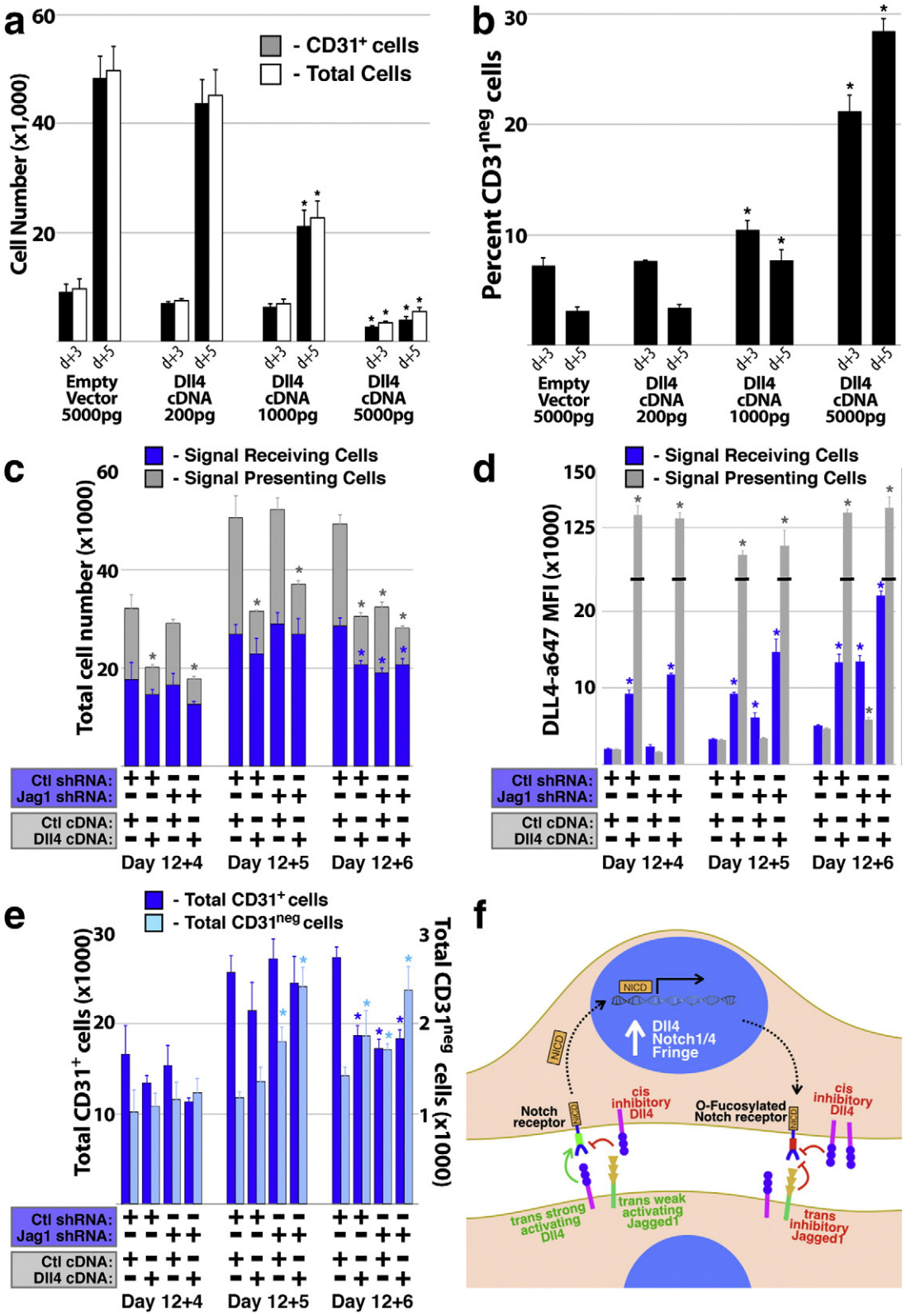


**Fig. 5.** Hyper-activation of Notch signaling promotes DLL4-mediated cis-inhibition and EndMT. (a and b) Following FACS isolation at day 14, hESC-ECs were transduced with lentiviral vectors driving constitutive expression of control (Empty) or DLL4 cDNA sequences; the number (a) and percentage (b) of $CD31^+$ cells was measured by flow cytometry for increasing viral titers of DLL4 cDNA at 3 and 5 days following addition of lentiviral particles. (c–e) hESC-ECs were isolated from either blank VPr-mOrange hESCs (signal presenting cells, grey) or VPr-mOrange hESCs that had been clonally labeled with BFP (signal receiving cells, blue); unlabeled ECs were transduced with control or DLL4 cDNA (500 pg titer), and $BFP^+$ ECs were transduced with control or JAG1 shRNAs. Equal numbers of signal presenting and signal receiving cells were combined and flow cytometry was used to quantify the total cell number (c), mean fluorescence intensity of surface DLL4 on ECs (d) and total $CD31^+$ and $CD31^{neg}$ cells (e) at 4, 5 and 6 days post co-culture. (f) Schematic model outlining feedback of Notch signal activation on elevated expression of Notch ligands/receptors and, ultimately, cis-inhibition in cells expressing high levels of DLL4. Error bars in (a–e) represent standard deviation of experimental values performed in triplicate; * - $p < 0.01$.

this was augmented by knockdown in JAG1 (Fig. 5e). Together, these results suggest that trans-activation of Notch signaling reduces EC expansion and, at high levels that are enabled by loss of JAG1 inhibitory function, promotes increased EndMT.

## 3. Discussion

During development, dysregulation of Notch signaling results in cardiovascular anomalies, and Notch signaling effectors are essential mediators of EndMT (Niessen and Karsan, 2008). Previous studies have identified inter-ligand competition (Benedito et al., 2009), post-translational modifications (Panin et al., 1997) and divergence in cis versus trans ligand activity (de Celis and Bray, 1997; Klein et al., 1997; Micchelli et al., 1997; Miller et al., 2009; Sprinzak et al., 2010) as modulators of Notch signal activation, yet few studies, to date, have interrogated the interplay of Notch ligands in the context of EndMT. Here, we have generated a hESC-derived EC population that is capable of recapitulating EndMT in monolayer culture, and utilized this platform to demonstrate a role for Notch signal hyper-activation in promoting EndMT. Trans-activation of Notch in hESC-derived ECs increased expression of DLL4 and NOTCH1/4, resulting in population level positive feedback in Notch activation. Competitive inhibition of Notch activation by JAG1 coincided with acquisition of mesenchymal phenotype, yet JAG1 knockdown promoted unrestrained activation of Notch signaling, upregulation of cis-inhibitory DLL4 and, ultimately, increased EndMT. These findings integrate a novel cellular mechanism of EndMT into the continuously evolving paradigm of Notch signaling during cardiovascular development and may contribute to therapeutic approaches for modulation of angiogenesis in regenerative and/or pathological contexts.

During vasculogenesis, the coupling of growth and patterning within the primitive vascular plexus is mediated by crosstalk between Notch and VEGF signaling. Activation of Notch in ECs results in downregulation of VEGFR2 (Taylor et al., 2002), thus restraining proliferation and inducing maturation in an angiogenic context. During retinal neovascularization, inhibition of Notch using DAPT results in enhanced EC sprouting and a dense vascular plexus (Benedito et al., 2009). Inhibition of Notch signaling has also been shown to augment yield of ECs during hESC differentiation (Sahara et al., 2015), with the benefit attributed to increased conversion of cardiovascular precursors to EC progenitors that have higher proliferative potential than mature ECs. Similarly, we show here that blockade of EC maturation via Notch inhibition can extend the proliferative lifespan of hESC-derived ECs, and we have elaborated a mechanism by which increased EC number derives, in part, from reduced EndMT.

Induction of EndMT results from integration of multiple extrinsic inputs within the dynamically shifting cellular environment of cardiogenesis. Owing to the membrane bound presentation of ligands, Notch signaling status is dependent on the organization and distribution of signal-presenting and signal-receiving cells. Conversely, the TGFβ pathway acts through a diversity of secreted morphogens, but has also been shown to play a pivotal role in EndMT (Gonzalez and Medici, 2014). Knockout of the type I receptor, ALK5, which responds to TGFβ1 ligand by activation of SMAD2/3, results in failure of EndMT induction from endocardium (Sridurongrit et al., 2008); and in hESC-derived ECs activation of SMAD2/3 induces phenotypic transition that can be mitigated by co-culture with the ALK4/5/7 inhibitor SB431542 (James et al., 2010). In this study, we found increased expression of BMPER, and decreased expression of endoglin in conditions that promote EndMT of hESC-derived ECs (Fig. 4f). BMPER antagonizes BMP signaling (Moser et al., 2003) and endoglin augments TGFβ signal activation by enabling ECs to respond to TGFβ1 ligand via activation of an ALK1:SMAD1/5/8 axis instead of a ALK5:SMAD2/3 axis (Lebrin et al., 2004). Hence, the shift from endoglin to BMPER expression in confluent hESC-ECs denotes a change from SMAD1/5/8 activation to SMAD2/3 activation, and may account, in part, for reduced EC number and increased EndMT. Indeed, ALK1 (Urness et al., 2000) or endoglin (Sorensen et al., 2003) loss of function in mice results in aberrant cardiac cushion formation and, in vitro, induces a shift in cultured ECs from proliferation to growth arrest (Lebrin et al., 2004). Our data revealed an increase in BMPER expression even in control conditions, but endoglin was uniquely reduced upon JAG1 knockdown. Although TGFβ signaling functions independently to promote EndMT, these results may reflect crosstalk between Notch and TGFβ signaling to enhance SMAD2/3 activation at the expense of SMAD1/5/8 activation.

Another pathway that has been linked to Notch is Nitric oxide (NO) signaling. NO signaling is a critical modulator of cardiac function (Rastaldo et al., 2007) and deficiency in NO generation in embryonic mice (Aicher et al., 2007; Feng et al., 2002; Lee et al., 2000) results in major cardiac anomalies that are similar to those displayed by human patients carrying Notch1 mutations (Garg et al., 2005). Chang et al. have linked Notch to activation of to an autocrine loop consisting of GUCY1A3, GUCY1B3, ACTIVINA and IGF2, which enables propagation of nitric oxide signaling, and ultimately EndMT in embryonic mouse heart (Chang et al., 2011). All of these factors were elevated in hESC-derived ECs under conditions that promoted EndMT (Fig. 4f), affirming that multiple signaling elements present during embryonic EndMT are recapitulated in our in vitro platform.

Despite being linked to multiple downstream effectors of EndMT, including NO signaling (Chang et al., 2011) and SLUG (Niessen et al., 2008), the molecular mechanisms that tip the balance of Notch signal activation leading up to EC trans-differentiation are not well defined. The increased surface expression of JAG1 observed in cells undergoing EndMT and coincident reduction in DLL4 expression (Fig. 3) suggested a role for JAG1 in attenuating Notch activation. Benedito et al. have demonstrated the role of JAG1 in designating tip versus stalk phenotype of ECs during retinal neo-vascularization (Benedito et al., 2009). In mice with EC-specific loss of JAG1, progression of the retinal vascular plexus is marked by reduced EC proliferation, elevated DLL4 expression and increased stalk to tip cell ratio. This phenotype arises from loss of JAG1-mediated Notch inhibition in ECs expressing Fringe genes. Similarly, our knockdown of JAG1 in hESC-derived ECs resulted in decreased cell counts and increased Notch activation/DLL4 expression, as well as increased EndMT. Although not emphasized in their study, Benedito et al. noted increased pericyte coverage and ectopic localization of vascular smooth muscle cells to venules in JAG1 loss-of-function mice. Because EC-specific loss of JAG1 in these mice may be partially rescued by surrounding non-endothelial cells, this phenotype may be a milder correlate to the effect observed in our in vitro platform, in which JAG1 loss of function was uniformly applied across a purified population of ECs.

The elevation of JAG1 surface expression in transitional ECs suggests that it plays a role in phenotypic transition of these cells. Overexpression of activated JAG1 cDNA in cultured human microvascular ECs activated a SMA-promoter driven luciferase and induced trans-differentiation to vascular smooth muscle cells (Noseda et al., 2004). Elevation of JAG1 during wound healing can function to attenuate activation of Notch signaling (Pedrosa et al., 2015) and expression profiling of $CD31^{+}$ ECs and $CD31^{neg}PDGFR\beta^{+}$ derivatives of EndMT revealed markedly reduced expression of genes related to Notch activation (Fig. 3e). Yet JAG1 is likely not the sole actor in reducing Notch pathway activation, as JAG1 knockdown leads to increased, instead of decreased EndMT. Here, we showed that increased Notch activation, as reflected by expression of Notch target DLL4, correlates with the degree of EndMT in hESC-EC monolayers (Fig. 5d and e). Previous work in Drosophila has identified the potential for Delta (DLL4 orthologue) to inhibit Notch on its own cell (de Celis and Bray, 1997; Klein et al., 1997; Micchelli et al., 1997; Miller et al., 2009), and Sprinzak et al. have modeled cis- and trans- activity of human DLL1-Notch1 in live cells using real time fluorescence microscopy (Sprinzak et al., 2010). This system revealed that while the response to trans-DLL1 is graded, inhibitory action of cis-DLL1 is sharp and occurs at a fixed threshold, irrespective of trans-DLL1 activity. Thus, JAG1 may contribute to attenuation of

Notch activation in hESC-ECs, but cis-inhibitory activity of DLL4 at a critical threshold of Notch hyper-activation likely accounts for the abrupt shift in Notch signaling status during EndMT.

Given the technical and bioethical hurdles associated with the study of human embryogenesis, a human cell-based model that approximates in vivo cardiogenesis provides unique insight into the cellular/molecular bases of cardiac anomalies. Moreover, mounting evidence supports a role for EndMT in wound healing and a broad array of pathological disease processes, including pulmonary (Arciniegas et al., 2005), intestinal (Rieder et al., 2011), cardiac (Zeisberg et al., 2007) and kidney fibrosis (Zeisberg et al., 2008). EndMT has also been identified as a critical mediator of neo-intima formation following coronary artery bypass grafting (Cooley et al., 2014) and has even been implicated in the advance of atherosclerosis in a mouse model of cardiovascular disease (Chen et al., 2015). Our results establish an in vitro model of embryonic EndMT using hESC-derived ECs, and utilize this platform to integrate EC membrane-bound Notch signaling inputs (DLL4) with pathway activation status and the initiation of EndMT. Understanding of the signaling mechanisms that regulate EC identity and its organization into multicellular vascular channels will be vital to implementing hESC-based vascular applications, and insight into molecular influences that mediate embryonic EndMT may provide fertile ground for therapeutic targeting of pathways that contribute to degenerative disease and organ/tissue fibrosis.

## 4. Materials and methods

### 4.1. Human ESC culture

Experiments in this report were performed using WMC-2 hESC (James et al., 2010). The permissions for use of these cell lines were obtained after comprehensive review by the Cornell-Rockefeller-Sloan Kettering Institute ESCRO committee. The funding for execution of these studies was secured from approved non-federal funding resources. Human ESC culture medium consisted of Advanced DMEM/F12 (Gibco) supplemented with 20% Knockout Serum Replacement (Invitrogen), 1× non-essential amino acids (Gibco), 1× L-Glutamine (Invitrogen), 1× Pen/Strep (Invitrogen), 1× β-Mercaptoethanol (Gibco), and 4 ng/ml FGF-2 (Invitrogen). Human ESCs were maintained on Matrigel™ using hESC medium conditioned by mouse embryonic fibroblasts (MEF, Chemicon).

### 4.2. Lentiviral vectors and transduction

The cDNA sequences for AdE4ORF1, DLL4 and BFP were cloned into the pCCL-PGK lentivirus vector. Scrambled, Dll1 and Jagged1 specific shRNA constructs were cloned into the pLKO vector. Lentivirus was generated by co-transfecting 15 μg of our gene of interest lentiviral vector, 3 μg of pENV/VSV-G, 5 μg of pRRE, and 2.5 μg of pRSV-REV in 293 T cells by the calcium precipitation method. Supernatants were collected 40 and 64 h after transfection as previously described (Naldini et al., 1996). Viral supernatants were concentrated by ultracentrifugation.

### 4.3. Generation of PGK-BFP/VPr-mOrange hESC lines

Two passages after addition of PGK-BFP lentiviral particles to VPr-mOrange hESCs, Accutase was used to form single cells, which were isolated and expanded in the presence of the ROCK inhibitor Y-27632 to form multiple parallel cultures and clones expressing clearly detectable levels of BFP were selected for experimentation.

### 4.4. EC feeder differentiation

VPr-mOrange hESCs were differentiation on vascular feeders as previously described (Rafii et al., 2013). Briefly, human umbilical vein endothelial cells were isolated and transduced with lentiviral AdE4ORF1 to generate durable PEC feeders (Seandel et al., 2008). One day in advance of plating hESCs on E4ORF1$^+$ primary human umbilical vein endothelial cells (PECs), MEF conditioned medium was replaced with hESC culture medium without FGF-2 and supplemented with 2 ng/ml BMP4. The next day, hESCs were onto an 80% confluent layer of E4ORF1$^+$ PEC in hESC culture medium (without FGF-2, plus 2 ng/ml BMP4) and left undisturbed for 48 h. At this point, cultures were considered as differentiation day zero and cells were sequentially stimulated with recombinant cytokines in the following order: day 0 to 7 supplemented with 10 ng/ml BMP4; day 2 to point of harvest supplemented with 10 ng/ml VEGF-A; day 2 to point of harvest supplemented with 5 ng/ml FGF-2; day 7 to point of harvest supplemented with 10 μM SB-431542, unless otherwise stated.

### 4.5. Flow cytometry and sorting

Flow cytometric analysis and sorting was performed on a FACS AriaII (BD). Antibodies used were specific for CD31 (BD), α-SMA (R&D) and DLL4 (Biolegend) and Jagged1 (R&D). Data was analyzed using FACS Diva software.

### 4.6. Quantitative PCR

Total RNA was prepared from cultured cells using the RNeasy extraction kit (Qiagen) and reverse transcribed using Quantitect Reverse Transcription Kit (Qiagen) according to the manufacturer's instructions. Relative quantitative PCR was performed on a 7500 Fast Real Time PCR System (Applied Biosystems) using SYBR Green PCR mix (Applied Biosystems). Human specific SYBR green primer pairs used were:

BMPER: f, 5′-aggacagtgctgccccaaatg-3′, r, 5′-tactgacacgtcccctgaaag-3′;

CALPONIN: f, 5′-gagtcaacccaaaattggcac-3′, r, 5′-ggactgcacctgtgtatggt-3′;

CD31: f, 5′-gacgtgctgttttacaacatctc-3′, r, 5′-cctcacgatcccaccttgg-3′;

COUP-TFII: f, 5′-ccgagtacagctgcctcaa-3′, r, 5′-ttttcctgcaagctttccac-3′;

DLL4: f, 5′-aactgcccttcaatttcacct-3′, r, 5′-gctggtttgctcatccaataa-3′;

ENDOGLIN: f, 5′-gaattctggtacatctactcgc-3′, r, 5′-ggctatgccatgctgctggtgg-3′;

EPHRINB2: f, 5′-ggactggtactatacccacagat-3′, r, 5′-tgtctgcttggtctttatcaacc-3′;

GAPDH: f, 5′-ctgatgcccccatgttcgtc-3′, r, 5′-caccctgttgctgtagccaaattc-3′;

GUCYA3: f, 5′-tacaaggtggagaccattggcgat-3′, r, 5′-atccagagtgcagtccaattcgca-3′;

GUCYB3: f, 5′-ggaaattgctggccaggttcaagt-3′, r, 5′-ttctcctgtggtttctgttcggct-3′;

HEY1 – f, 5′-gtgcggacgagaatggaaa-3′, r, 5′-ctggccaaaatctgggaaga-3′;

IGF2: f, 5′-acaccctccagttcgtctgt-3′, r, 5′-gaaacagcactcctcaacga-3′;

INHIBINA: f, 5′-ctcggagatcatcacgtttg-3′, r, 5′-ccttggaaatctcgaaagtgc-3′;

JAGGED1: f, 5′-caacacggtccccatcaag-3′, r, 5′-tacttcagaattgtgtgtcctatttt-3′;

JAGGED2: f, 5′-ggtcgtacttgcactcacaatacc-3′, r, 5′-gtagcaaggcagagggttgc-3′;

NOTCH1: f, 5′-ccgcagttgtgctcctgaa-3′, r, 5′-accttggcggtctcgtagct-3′;

NOTCH3: f, 5′-tccagattctcatccgaaaccgct-3′, r, 5′-gggtctcctccttgctatcctgcat-3′;

NOTCH4: f, 5′-cccaggaatctgagatggaa-3′, r, 5′-ccacagcaaactgctgacat-3′;

PDGFRβ – f, 5′-agacacgggagaatacttttgc-3′, r, 5′-agttcctcggcatcattaggg-3′;

SLUG: f, 5′-agatgcatattcggacccac-3′, r, 5′-cctcatgtttgtgcaggaga-3′;

VE-CADHERIN – f, 5′-tggagaagtggcatcagtcaacag-3′, r, 5′-tctacaatcccttgcagtgtgag-3′;

VEGFR2: f, 5′-actttggaagacagaaccaaattatctc-3′, r, 5′-tgggcaccattccacca-3′;

qPCR Primers specific for Lunatic and Manic Fringe were obtained from Origene. Cycle conditions were: one cycle at 50 °C for 2 min; 1 cycle at 95 °C for 10 min; 40 repeat cycles followed by 95 °C for 15 s

and 60 °C for 1 min. Threshold cycles of primer probes were normalized to the housekeeping gene β-Actin and translated to relative values.

### 4.7. Immunofluorescence

Cells were immunocytochemically stained as previously described (James et al., 2010). Briefly, samples were permeabilized in PBST and blocked in 5% donkey serum. Samples were incubated for 2 h in primary antibodies blocking solution, washed 3 times in PBS and incubated in secondary antibodies (Jackson Laboratories) for 1 h. Following washing some sections were counterstained for nucleic acids by DAPI (Invitrogen) before mounting and imaging by confocal microscopy. The Primary antibodies used for immunostaining were CD31 (BD), PDGFRβ (BD), α-SMA (R&D), JAGGED1 (R&D), HEY1 (R&D) and NOTCH1-ICD (R&D). All imaging was performed using a Zeiss 710 META confocal microscope.

Supplementary data to this article can be found online at http://dx.doi.org/10.1016/j.scr.2016.09.005.

## References


Aicher, D., Urbich, C., Zeiher, A., Dimmeler, S., Schafers, H.J., 2007. Endothelial nitric oxide synthase in bicuspid aortic valve disease. Ann. Thorac. Surg. 83, 1290–1294.

Arciniegas, E., Neves, C.Y., Carrillo, L.M., Zambrano, E.A., Ramirez, R., 2005. Endothelial-mesenchymal transition occurs during embryonic pulmonary artery development. Endothelium 12, 193–200.

Benedito, R., Roca, C., Sorensen, I., Adams, S., Gossler, A., Fruttiger, M., Adams, R.H., 2009. The notch ligands DLL4 and Jagged1 have opposing effects on angiogenesis. Cell 137, 1124–1135.

Chang, A.C., Fu, Y., Garside, V.C., Niessen, K., Chang, L., Fuller, M., Setiadi, A., Smrz, J., Kyle, A., Minchinton, A., et al., 2011. Notch initiates the endothelial-to-mesenchymal transition in the atrioventricular canal through autocrine activation of soluble guanylyl cyclase. Dev. Cell 21, 288–300.

Chen, P.Y., Qin, L., Barnes, C., Charisse, K., Yi, T., Zhang, X., Ali, R., Medina, P.P., Yu, J., Slack, F.J., et al., 2012. FGF regulates TGF-beta signaling and endothelial-to-mesenchymal transition via control of let-7 miRNA expression. Cell Rep. 2, 1684–1696.

Chen, P.Y., Qin, L., Baeyens, N., Li, G., Afolabi, T., Budatha, M., Tellides, G., Schwartz, M.A., Simons, M., 2015. Endothelial-to-mesenchymal transition drives atherosclerosis progression. J. Clin. Invest. 2015.

Cooley, B.C., Nevado, J., Mellad, J., Yang, D., St Hilaire, C., Negro, A., Fang, F., Chen, G., San, H., Walts, A.D., et al., 2014. TGF-beta signaling mediates endothelial-to-mesenchymal transition (EndMT) during vein graft remodeling. Sci. Transl. Med. 6, 227ra234.

de Celis, J.F., Bray, S., 1997. Feed-back mechanisms affecting Notch activation at the dorsoventral boundary in the Drosophila wing. Development 124, 3241–3251.

Feng, Q., Song, W., Lu, X., Hamilton, J.A., Lei, M., Peng, T., Yee, S.P., 2002. Development of heart failure and congenital septal defects in mice lacking endothelial nitric oxide synthase. Circulation 106, 873–879.

Garg, V., Muth, A.N., Ransom, J.F., Schluterman, M.K., Barnes, R., King, I.N., Grossfeld, P.D., Srivastava, D., 2005. Mutations in NOTCH1 cause aortic valve disease. Nature 437, 270–274.

Gonzalez, D.M., Medici, D., 2014. Signaling mechanisms of the epithelial-mesenchymal transition. Sci. Signal. 7, re8.

Guruharsha, K.G., Kankel, M.W., Artavanis-Tsakonas, S., 2012. The Notch signalling system: recent insights into the complexity of a conserved pathway. Nat. Rev. Genet. 13, 654–666.

Harvey, R.P., 2002. Patterning the vertebrate heart. Nat. Rev. Genet. 3, 544–556.

James, D., Nam, H.S., Seandel, M., Nolan, D., Janovitz, T., Tomishima, M., Studer, L., Lee, G., Lyden, D., Benezra, R., et al., 2010. Expansion and maintenance of human embryonic stem cell-derived endothelial cells by TGFbeta inhibition is Id1 dependent. Nat. Biotechnol. 28, 161–166.

James, D., Zhan, Q., Kloss, C., Zaninovic, N., Rosenwaks, Z., Rafii, S., 2011. Lentiviral transduction and clonal selection of hESCs with endothelial-specific transgenic reporters. Curr. Protoc. Stem Cell Biol. (Chapter 1, Unit1F 12).

Klein, T., Brennan, K., Arias, A.M., 1997. An intrinsic dominant negative activity of serrate that is modulated during wing development in Drosophila. Dev. Biol. 189, 123–134.

Lebrin, F., Goumans, M.J., Jonker, L., Carvalho, R.L., Valdimarsdottir, G., Thorikay, M., Mummery, C., Arthur, H.M., ten Dijke, P., 2004. Endoglin promotes endothelial cell proliferation and TGF-beta/ALK1 signal transduction. EMBO J. 23, 4018–4028.

Lee, T.C., Zhao, Y.D., Courtman, D.W., Stewart, D.J., 2000. Abnormal aortic valve development in mice lacking endothelial nitric oxide synthase. Circulation 101, 2345–2348.

Micchelli, C.A., Rulifson, E.J., Blair, S.S., 1997. The function and regulation of cut expression on the wing margin of Drosophila: Notch, Wingless and a dominant negative role for Delta and Serrate. Development 124, 1485–1495.

Miller, A.C., Lyons, E.L., Herman, T.G., 2009. cis-Inhibition of Notch by endogenous Delta biases the outcome of lateral inhibition. Curr. Biol. 19, 1378–1383.

Moser, M., Binder, O., Wu, Y., Aitsebaomo, J., Ren, R., Bode, C., Bautch, V.L., Conlon, F.L., Patterson, C., 2003. BMPER, a novel endothelial cell precursor-derived protein, antagonizes bone morphogenetic protein signaling and endothelial cell differentiation. Mol. Cell. Biol. 23, 5664–5679.

Naldini, L., Blomer, U., Gallay, P., Ory, D., Mulligan, R., Gage, F.H., Verma, I.M., Trono, D., 1996. In vivo gene delivery and stable transduction of nondividing cells by a lentiviral vector. Science 272, 263–267.

Niessen, K., Karsan, A., 2008. Notch signaling in cardiac development. Circ. Res. 102, 1169–1181.

Niessen, K., Fu, Y., Chang, L., Hoodless, P.A., McFadden, D., Karsan, A., 2008. Slug is a direct Notch target required for initiation of cardiac cushion cellularization. J. Cell Biol. 182, 315–325.

Noseda, M., McLean, G., Niessen, K., Chang, L., Pollet, I., Montpetit, R., Shahidi, R., Dorovini-Zis, K., Li, L., Beckstead, B., et al., 2004. Notch activation results in phenotypic and functional changes consistent with endothelial-to-mesenchymal transformation. Circ. Res. 94, 910–917.

Panin, V.M., Papayannopoulos, V., Wilson, R., Irvine, K.D., 1997. Fringe modulates Notch-ligand interactions. Nature 387, 908–912.

Parks, A.L., Klueg, K.M., Stout, J.R., Muskavitch, M.A., 2000. Ligand endocytosis drives receptor dissociation and activation in the Notch pathway. Development 127, 1373–1385.

Pedrosa, A.R., Trindade, A., Fernandes, A.C., Carvalho, C., Gigante, J., Tavares, A.T., Dieguez-Hurtado, R., Yagita, H., Adams, R.H., Duarte, A., 2015. Endothelial Jagged1 antagonizes DLL4 regulation of endothelial branching and promotes vascular maturation downstream of DLL4/Notch1. Arterioscler. Thromb. Vasc. Biol. 35, 1134–1146.

Rafii, S., Kloss, C.C., Butler, J.M., Ginsberg, M., Gars, E., Lis, R., Zhan, Q., Josipovic, P., Ding, B.S., Xiang, J., et al., 2013. Human ESC-derived hemogenic endothelial cells undergo distinct waves of endothelial to hematopoietic transition. Blood 121, 770–780.

Rastaldo, R., Pagliaro, P., Cappello, S., Penna, C., Mancardi, D., Westerhof, N., Losano, G., 2007. Nitric oxide and cardiac function. Life Sci. 81, 779–793.

Rieder, F., Kessler, S.P., West, G.A., Bhilocha, S., de la Motte, C., Sadler, T.M., Gopalan, B., Stylianou, E., Fiocchi, C., 2011. Inflammation-induced EndMT: a novel mechanism of intestinal fibrosis. Am. J. Pathol. 179, 2660–2673.

Sahara, M., Hansson, E.M., Wernet, O., Lui, K.O., Spater, D., Chien, K.R., 2015. Manipulation of a VEGF-Notch signaling circuit drives formation of functional vascular endothelial progenitors from human pluripotent stem cells. Cell Res. 25, 148.

Seandel, M., Butler, J.M., Kobayashi, H., Hooper, A.T., White, I.A., Zhang, F., Vertes, E.L., Kobayashi, M., Zhang, Y., Shmelkov, S.V., et al., 2008. Generation of a functional and durable vascular niche by the adenoviral E4ORF1 gene. Proc. Natl. Acad. Sci. U. S. A. 105, 19288–19293.

Sorensen, L.K., Brooke, B.S., Li, D.Y., Urness, L.D., 2003. Loss of distinct arterial and venous boundaries in mice lacking endoglin, a vascular-specific TGFbeta coreceptor. Dev. Biol. 261, 235–250.

Sprinzak, D., Lakhanpal, A., Lebon, L., Santat, L.A., Fontes, M.E., Anderson, G.A., Garcia-Ojalvo, J., Elowitz, M.B., 2010. Cis-interactions between Notch and Delta generate mutually exclusive signalling states. Nature 465, 86–90.

Sridurongrit, S., Larsson, J., Schwartz, R., Ruiz-Lozano, P., Kaartinen, V., 2008. Signaling via the Tgf-beta type I receptor Alk5 in heart development. Dev. Biol. 322, 208–218.

Taylor, K.L., Henderson, A.M., Hughes, C.C., 2002. Notch activation during endothelial cell network formation in vitro targets the basic HLH transcription factor HESR-1 and downregulates VEGFR-2/KDR expression. Microvasc. Res. 64, 372–383.

Urness, L.D., Sorensen, L.K., Li, D.Y., 2000. Arteriovenous malformations in mice lacking activin receptor-like kinase-1. Nat. Genet. 26, 328–331.

von Gise, A., Pu, W.T., 2012. Endocardial and epicardial epithelial to mesenchymal transitions in heart development and disease. Circ. Res. 110, 1628–1645.

Zeisberg, E.M., Tarnavski, O., Zeisberg, M., Dorfman, A.L., McMullen, J.R., Gustafsson, E., Chandraker, A., Yuan, X., Pu, W.T., Roberts, A.B., et al., 2007. Endothelial-to-mesenchymal transition contributes to cardiac fibrosis. Nat. Med. 13, 952–961.

Zeisberg, E.M., Potenta, S.E., Sugimoto, H., Zeisberg, M., Kalluri, R., 2008. Fibroblasts in kidney fibrosis emerge via endothelial-to-mesenchymal transition. J. Am. Soc. Nephrol. 19, 2282–2287.